Texture investigation of the superelastic Ti-24Nb-4Zr-8Sn alloy

Y. Yang, Philippe Castany, Maryline Cornen, I. Thibon, F. Prima, Thierry Gloriant

Texture investigation of the superelastic Ti-24Nb-4Zr-8Sn alloy

Y. YANG[1], P. CASTANY[1*], M. CORNEN[1], I. THIBON[1], F. PRIMA[2], T. GLORIANT[1]

[1] *INSA Rennes, UMR CNRS 6226 ISCR, Laboratoire Chimie-Métallurgie, 20 avenue des Buttes de Coësmes, 35708 Rennes, France*

[2] *Laboratoire de Physico-Chimie des surfaces, Groupe de Métallurgie Structurale (UMR 7045), Chimie-ParisTech, Paris, France*

Abstract

In this work, the influence of crystallographic texture on mechanical properties was investigated by X-ray diffraction in the superelastic Ti-24Nb-4Zr-8Sn alloy. Different textures were obtained by changing the cold rolling reduction rate and the following thermal treatment (solution treatment or flash thermal treatment). The tensile tests performed show that Young's modulus, elongation at rupture and ultimate tensile strength are not influenced by texture. However, the superelastic property of the Ti-24Nb-4Zr-8Sn alloy after solution treatment clearly increases with the textural change into the γ-fiber texture with a $(111)[1\bar{2}1]$ main component due to the increase of cold rolling rate. Contrarily, the texture change induced by the increase of cold rolling rate has no influence on superelasticity after flash thermal treatment. Flash thermal treatment gives also higher recovery strain than solution treatment due to a smaller grain size.

Keywords: Texture; Superelasticity; Titanium alloy; Tensile tests.

1. Introduction

The Ti-24Nb-4Zr-8Sn alloy (Ti2448 for short later in this paper) is a new β-type multifunctional alloy (body-centered cubic structure). This alloy displays interesting properties such as high strength, low elastic modulus, high ductility, superelastic property and good biocompatibility. In previous works, different kinds of thermo-mechanical treatments were used for the processing of the alloy (cold deformation, hot rolling and warm rolling) [1-6]. Thanks to these investigations, a superelasticity of about 3.3% was obtained [3-6], which is much higher than the values usually obtained with binary Ti-Nb alloys [7-9]. Moreover, " flash treatments " (thermal treatment at 700°C for 3min for example) carried out on the as-cold rolled Ti2448 alloy allow to further enhance the superelastic property, combined with a very high strength in that case [10]. These properties were recently correlated to the reduced grain size, which is due to the strong applied plastic deformation combined with the following rapid recrystallization treatment in the β phase field [10]. Furthermore, intense plastic deformation is known to induce strong crystallographic texture, which can also influence the mechanical properties and, in the present case, the superelastic behavior of the Ti2448 alloy. As for example, texture evolution after warm rolling was previously investigated in detail in a β titanium alloy [11] and it was evaluated that the superelastic recovery strain is maximized for grains strained along $<110>$ direction [7]. Consequently, a control of the texture can also be used in order to improve the superelasticity of β titanium alloys [7, 12].

In this work, moderate, intermediate and high cold rolling reduction rates were used in the Ti2448 alloy in order to vary the crystallographic texture in its solution treated state and after flash thermal treatment. The influence of the resulting texture on the related mechanical properties (tensile strength, Young's modulus, superelastic recovery strain) was investigated in detail.

2. Experiments

A hot-forged Ti2448 cylinder with diameter of 55 mm was used as raw material

in this work. The chemical composition of the alloy is given in Table 1. Hot-forged slice-cut samples were directly multi-pass cold rolled without intermediate annealing to reach the final thickness of 0.5 mm. According to different initial thicknesses of the samples used, three reduction rates were obtained: 40% (moderate), 80%(intermediate) and 94% (high). For each reduction rate, two thermal treatments were performed: on the one hand, cold rolled specimens were solution treated under high vacuum at 900 °C for 30 minutes followed by water quenching (solution treated state, ST); on the other hand, cold rolled specimens were thermally "flash treated" at 700 °C for 3 minutes followed by air cooling (flash treated state, FT). After thermal treatments, all specimens were cleaned in an acid solution made of 50% HF and 50% HNO_3 (in volume) to remove any oxidation layer. Each specimen is labeled as CR*XX*%-ST and CR*XX*%-FT depending if a solution treatment (ST) or a flash thermal treatment (FT) was performed and where *XX*% mentions the applied cold rolling rate.

Mechanical properties and superelasticity were estimated by conventional and cyclic tensile tests with a strain rate of 10^{-4} s^{-1}. Cyclic tensile tests consist of strain increments of 0.5% followed by stress release up to an elongation of 5%. An extensometer was used to ensure the accuracy of strain. Normalized flat tensile specimens with 3mm×15mm×0.5mm gage dimensions were used. The tensile direction was chosen parallel to the rolling direction.

Microstructure was characterized by optical microscopy. Prior to observations, samples were first mechanically polished and next chemically etched with a 15% HNO_3, 8% HF and 77% H_2O solution (vol.%). Transmission electron microscopy (TEM) was also used to characterize the smaller microstructure of FT specimens. Samples were thinned down using a twin-jet electropolishing system with a solution of 4% perchloric acid and 96% methanol (vol.%).

Phase and texture analysis based on X-ray diffraction were conducted on a Philips PW3710 system with Cu-$K\alpha_1$ radiation (λ = 0.154060 nm). For texture analysis, the sample coordinate system was defined as rolling direction (RD), normal direction (ND) and transverse direction (TD). The step size used for the data

acquisition is 5º. Orientation Distribution Functions (ODF) were calculated with the raw data of the most important three pole figures (110), (200) and (211) after applying corrections for background and defocusing. Contoured plots of ODF were delineated for constant φ_2 sections in the volume of the reduced Euler space ($0°<\varphi_1, \phi, \varphi_2<90°$).

3. Results and discussion

3.1. Microstructure and phase constitution

The X-ray diffraction patterns of Ti-24Nb-4Zr-8Sn are shown in Fig. 1.Whatever the reduction rate and the thermal treatment applied, only a full-recrystallized β phase microstructure was obtained. Indeed, only (110), (200), (211), and (220) peaks of the body-centered cubic (bcc) β phase are observed. The lattice parameter of β phase is calculated to be close to 0.3292nm, which is consistent with the results published previously for the Ti2448 alloy [13]. The microstructure consists of equiaxed grains after solution treatment (Fig. 2a to 2c) with an average grain size of 60 μm for CR40% and 50 μm for both CR80% and CR94%. After flash thermal treatment, optical micrographs reveal similar microstructures for each cold rolling rate with smaller grains whose size is measured lesser than 10 μm (Fig. 2d to 2f). However, TEM observations show that the grain size is smaller than what is observed in optical micrographs for the flash thermal treated alloy. The grain size is observed to be independent of the applied cold rolling rate and the microstructures are similar: for example, Fig. 3 illustrates the microstructure with sub-micron grains of the CR94%-FT specimen. For each thermal treatment (ST or FT), the grain size is thus almost independent of the cold rolling rate.

3.2. Mechanical properties

Fig. 4 displays the conventional and cyclic tensile curves obtained after different thermo-mechanical treatments. In Table 2, the mechanical characteristics determined from tensile tests (elongation at rupture, ultimate tensile strength and incipient Young's modulus) are reported.

Elongation at rupture was evaluated to lie between 8% and 13% and no clear difference in ductility was observed whatever the applied thermo-mechanical process.

From the conventional tensile curves (Fig. 4a and 4b), a double yielding phenomenon associated to the superelastic property of this alloy is clearly observed, suggesting that α" martensitic transformation has occurred [7, 8]. For both thermal treatments, no clear influence of reduction rate on mechanical properties can be noticed, except for the CR94%-FT sample, where a slight increase of about 50 MPa in ultimate tensile strength can be observed (Fig. 4b and Table 2). However, a strengthening effect can be clearly observed after the flash thermal treatment (Table 2) since higher ultimate tensile strength of about 100 MPa is obtained by comparison to the solution treated alloy. This strengthening effect can be explained by the reduction of the grain size after flash thermal treatment (Fig. 2 and Fig. 3), which was also observed in recent works after similar flash thermal treatment [10, 14] or warm rolling [1, 2, 4], in comparison with the large grain size (several tens of micrometers) obtained after solution treatment.

The cyclic stress-strain curves, between 0 and 5% of strain, are given in Fig. 4c and 4d. All tensile curves display hysteresis loops between loading and unloading, which are due to the reversible stress-induced martensitic transformation. For each cycle, the recovery strain as a function of the applied strain is plotted in Fig. 5 in order to evaluate the evolution of the elastic recovery. As it can be seen on this figure, the most important influential factor is the thermal treatment. Indeed, the highest recovery strain (2.75%) is obtained for the flash treated samples while "only" 2% maximum are reached for the solution treated specimens (at 3.5% of applied strain). It seems also that the maximum recovery strain is enhanced by the increase of cold rolling reduction rate as well, particularly for the solution treated samples.

3.3. Texture evaluation

Fig. 6 shows the different ODF obtained on samples after thermo-mechanical treatments: Fig. 6a to 6c for the solution treated samples and Fig. 6d to 6f for the flash

thermal treated samples after 40%, 80% and 94% of cold rolling reduction rate, respectively.

After solution treatment, the CR40%-ST sample (Fig. 6a) does not show a strong texture but the main component $(01\bar{1})[100]$ (0°, 45°, 0°) can clearly be identified. For higher reduction rate (CR80%-ST, Fig. 6b), it can be observed preferential orientations on the γ-fiber. The γ-fiber is defined as containing all orientations of $(111)<uvw>$ type and can be visible on the φ_2=45° section where ϕ=55°. For more precision, the orientation densities are drawn in Fig. 7 with variable φ_1 angle. At intermediate cold rolling rate (Fig. 6b), the texture concentrates mainly on the γ-fiber, that is all the grains are oriented so that a {111} plane is parallel to the surface of the sample. This γ-fiber is commonly observed in bcc alloys [15-17] and was recently observed in β-titanium alloys after high deformation reduction rates [11]. At high cold rolling rate (CR94%-ST, Fig. 6c) the same observation can be obtained, but the component $(11\bar{1})[1\bar{2}1]$ appears prominent on this same fiber.

After flash thermal treatment, the lowest cold rolling rate (CR40%-FT, Fig. 6d) exhibits a clear texture corresponding mainly to $(21\bar{1})[0\bar{1}1]$ (50°, 66°, 63°). With the CR80%-FT sample (Fig. 6e), this orientation remains but orientations along the γ-fiber are also observed as the same shown in the solution treated samples. For the CR94%-FT, only orientations of the γ-fiber are observed (Fig. 6f). It seems that higher the reduction rate is, stronger the γ-fiber is as seen on Fig. 7 wherein the intensity of orientations along this fiber increases with the cold rolling rate. For both thermal treatments, the main component of the γ-fiber is $(11\bar{1})[1\bar{2}1]$ after high cold rolling rate, but with a stronger intensity for the solution treated samples.

3.4. Relationship between texture and mechanical properties

For solution treated samples, an increase of the superelasticity is observed by increasing the cold rolling rates (Fig. 5). It was shown previously that the recovery strain due to the reversible stress-induced martensitic transformation is maximum

when the grains are orientated with a $<110>$ direction parallel to the tensile direction [7]: indeed, when the bcc lattice of the β phase transforms to the orthorhombic lattice of the α" martensite, the maximum transformation strain is obtained along the <110> directions of the bcc lattice. In turn, the recovery strain due to the stress-induced martensitic transformation in a polycrystal will increase when the number of grains with <110> directions along the tensile direction increases. In the present ST samples, this optimal condition is fulfilled only at higher cold rolling rates (80% and 94%) since the $(11\bar{1})[1\bar{1}0]$ orientation is along the γ-fiber. Moreover, there is a higher density of this specific orientation by increasing the cold rolling rate (Fig. 7). The increase of the superelasticity in ST samples can thus be linked to the higher amount of grains processing the appropriated orientation due to the texture evolution when the cold rolling rate is increased.

For the flash thermal treated samples, no change in superelasticity is observed whatever the cold rolling rate (Fig. 5). Consequently, the texture change observed from 40% to 94% of reduction rate does not influence the superelastic recovery strain. This is due to the fact that, for each cold rolling rate, there is always the same significant amount of grains processing the favorable orientation that are $(21\bar{1})[0\bar{1}1]$ and $(11\bar{1})[1\bar{1}0]$ along the γ-fiber for the former (Fig. 6 and 7). Additionally, grains with other orientations exhibit lower recovery strain and have thus a weaker influence on superelasticity [7]. As a consequence, the change in texture does not influence noticeably the strain recovered by the martensitic transformation, which is so independent on the cold rolling rate after flash thermal treatment.

By comparing FT and ST samples, a strong increase of the superelasticity is observed as previously mentioned (Fig. 5). At least for both higher cold rolling rates (80% and 94%), it is clear that this increase cannot be attributed to the texture as both samples exhibit the same γ-fiber texture but a different recovery strain. This increase for the FT samples can thus rather be due to the reduced grain size as reported in previous work [10, 14]. Indeed, the stress-induced martensite can be trapped by

dislocations, which can impede a total reversion during the unloading. That means the volume fraction of martensite and the transformation strain would be similar for both thermal treatments, but the reverse transformation during unloading is impeded by dislocations for ST samples whereas a smaller density of dislocations in FT samples allows the reversion of the transformation to be more complete. An increase of the critical stress of dislocation slip, obtained by a smaller grain size, can thus improve the superelastic behavior of FT samples.

About the relationship between texture and superelasticity, one can conclude that after solution treatment, superelasticity increases by increasing cold rolling rate due to an evolution of texture. Contrarily, the change in texture after flash thermal treatment does not affect the superelasticity because there is no significant change of the amount of grains ideally orientated for the martensitic transformation. Finally, FT samples exhibit higher recovery strain than ST samples due to a smaller grain size that rises up the critical stress of dislocation slip and thus allow a better reversibility of the stress-induced martensitic transformation.

4. Conclusion

Texture evaluation and its relationship with superelasticity have been investigated for the Ti2448 alloy with three cold rolling reduction rates (40%, 80% and 94%) and two following thermal treatments (ST and FT) in this work. The main conclusions are:

- For ST samples, the main orientation is $(011)[100]$ at moderate cold rolling rate (40%) whereas a γ-fiber texture is observed at higher cold rolling rates (80% and 94%) with the $(111)[1\bar{2}1]$ orientation as a main component (CR94%-ST).

- For FT samples, a γ-fiber texture with the $(111)[1\bar{2}1]$ main component is observed at intermediate (80%) and high (94%) cold rolling rates. But a clear texture corresponding mainly to $(211)[0\bar{1}1]$ is obtained after a moderate cold rolling rate (40%).

- FT samples exhibit higher ultimate tensile strength than ST samples due to a smaller grain size. Young' modulus and elongation at rupture are shown to be independent of the applied thermo-mechanical process and thus of the texture, contrarily to superelasticity.

- Superelasicity of ST samples increases with the cold rolling rate in relation with the texture change. Indeed, the amount of grains orientated to give the highest recovery strain, that are with $<110>$ directions along the tensile direction, increases with the cold rolling rate.

- Superelasicity of FT samples is not influenced by the texture change due to the variation of cold rolling rate because the amount of grains orientated to give the highest recovery strain does not vary significantly.

- FT samples exhibit better superelasticity than ST samples. For both higher cold rolling rates (80% et 94%), the higher superelastic properties observed with the FT samples cannot be correlated to the texture but are clearly due to the grain refinement.

Acknowledgment

This work was financially supported by China scholarship Council (CSC), with No. 2011-6031.

References

[1] Y.L. Hao, S.J. Li, S.Y. Sun, C.Y. Zheng, Q.M. Hu, R. Yang, Appl. Phys. Lett. 87 (2005) 091906.

[2] Y.L. Hao, S.J. Li, B.B. Sun, M.L. Sui, R. Yang, Phys. Rev. Lett. 98 (2007) 216405.

[3] S.J. Li, T.C. Cui, Y.L. Li, Y.L. Hao, R. Yang, Appl. Phys. Lett. 92 (2008) 043128.

[4] S.J. Li, M.T. Jia, F. Prima, Y.L. Hao, R. Yang, Scripta Mater. 64 (2011) 1015-1018.

[5] Y.L. Hao, Z.B. Zhang, S.J. Li, R. Yang, Acta Mater. 60 (2012) 2169-2177.

[6] Y.L. Hao, S.J. Li, S.Y. Sun, C.Y. Zheng, R. Yang, Acta Biomater. 3 (2007)

277-286.

[7] H.Y. Kim, T. Sasaki, K. Okutsu, J.I. Kim, T. Inamura, H. Hosoda, S. Miyazaki, Acta Mater. 54 (2006) 423-433.

[8] H.Y. Kim, Y. Ikehara, J.I. Kim, H. Hosoda, S. Miyazaki, Acta Mater. 54 (2006) 2419-2429.

[9] A. Ramarolahy, P. Castany, F. Prima, P. Laheurte, I. Péron, T. Gloriant, J. Mech. Behav. Biomed. Mater. 9 (2012) 83-90.

[10] F. Sun, S. Nowak, T. Gloriant, P. Laheurte, A. Eberhardt, F. Prima, Scripta Mater. 63 (2010) 1053-1056.

[11] B. Sander, D. Raabe, Mater. Sci. Eng. A 479 (2008) 236-247.

[12] E. Bertrand, P. Castany, T. Gloriant, Acta Mater. 61 (2013) 511-518.

[13] Y.L. Hao, S.J. Li, S.Y. Sun, R. Yang, Mater. Sci. Eng. A 441 (2006) 112-118.

[14] F. Sun, Y.L. Hao, S. Nowak, T. Gloriant, P. Laheurte, F. Prima, J. Mech. Behav. Biomed. Mater. 4 (2011) 1864-1872.

[15] D. Raabe, K. Lücke, Mater. Sci. Technol. 9 (1993) 302–312.

[16] M. Hölscher, D. Raabe, K. Lücke, Acta Metall. 42 (1994) 879–886.

[17] D. Raabe, Mater. Sci. Technol. 11 (1995) 461–468.

Table 1. Chemical composition of hot forged Ti2448 (wt%).

Nb	Zr	Sn	O	Ti
23.9	4.05	8.22	0.16	Bal.

Table 2. Mechanical properties of solution treated and flash thermal treated Ti2448 alloy after different cold rolling rates.

Reduction rate/%	Elongation at rupture/%		Ultimate tensile strength/MPa		Young's modulus/GPa	
	ST	FT	ST	FT	ST	FT
CR40%	10	9	873	944	58	58
CR80%	12	8	868	954		
CR94%	13	9	877	990		

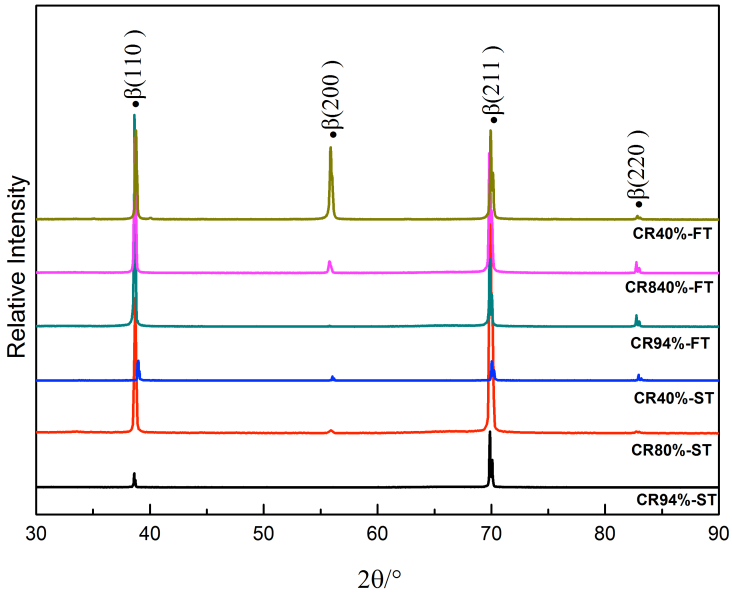

Fig. 1. XRD profiles of Ti2448 alloy after different thermo-mechanical treatments.

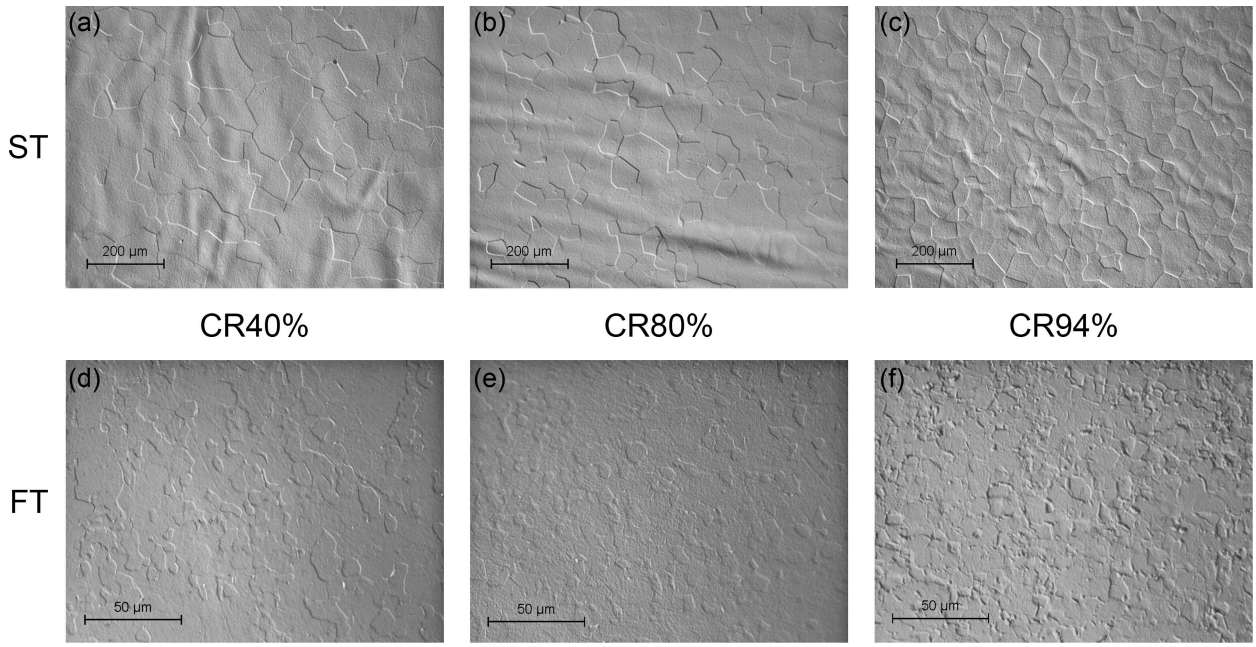

Fig. 2. Optical micrographs of Ti2448 after different cold rolling rates and solution treatment ST (a to c) or flash thermal treatment FT (d to f), respectively.

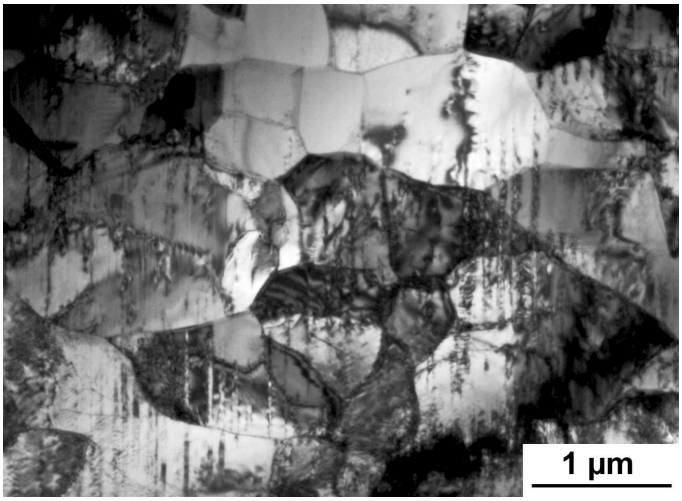

Fig. 3. Bright-field TEM micrograph after cold rolling rate of 94% followed by flash thermal treatment showing sub-micron grains. The same microstructure is observed for each cold rolling rate after flash thermal treatment.

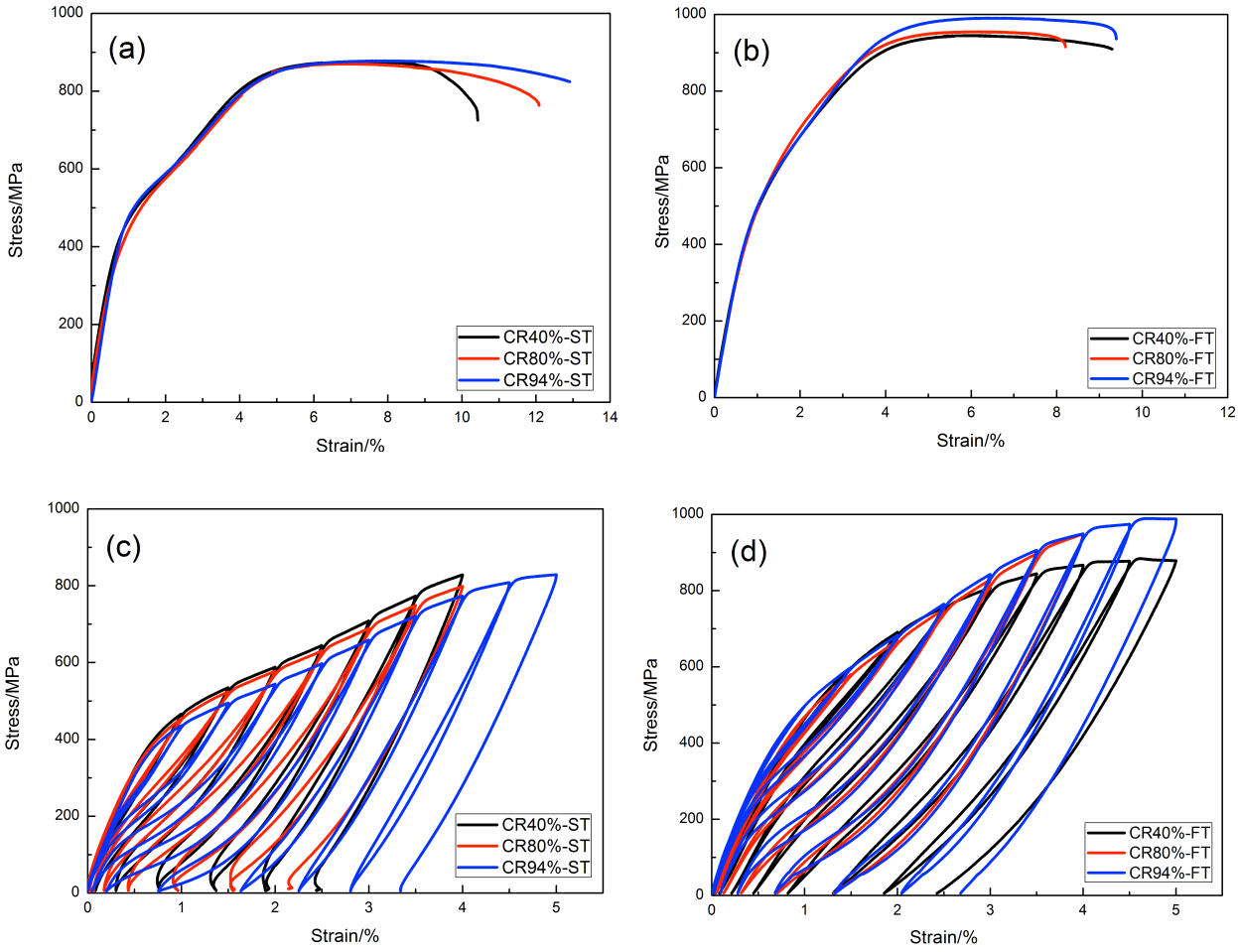

Fig. 4. Stress-strain curves obtained from conventional and cyclic tensile tests for Ti2448 alloy after different cold rolling rates followed by solution treatment at 900°C for 30min (a and c) or flash treatment at 700°C for 3min (b and d).

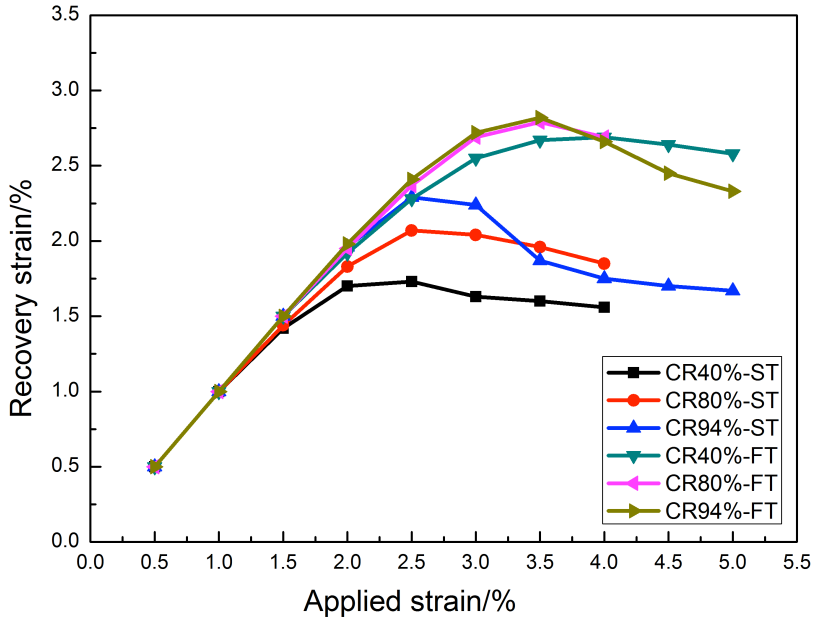

Fig. 5. Variation of recovery strain for different thermo-mechanical conditions of Ti2448 alloy.

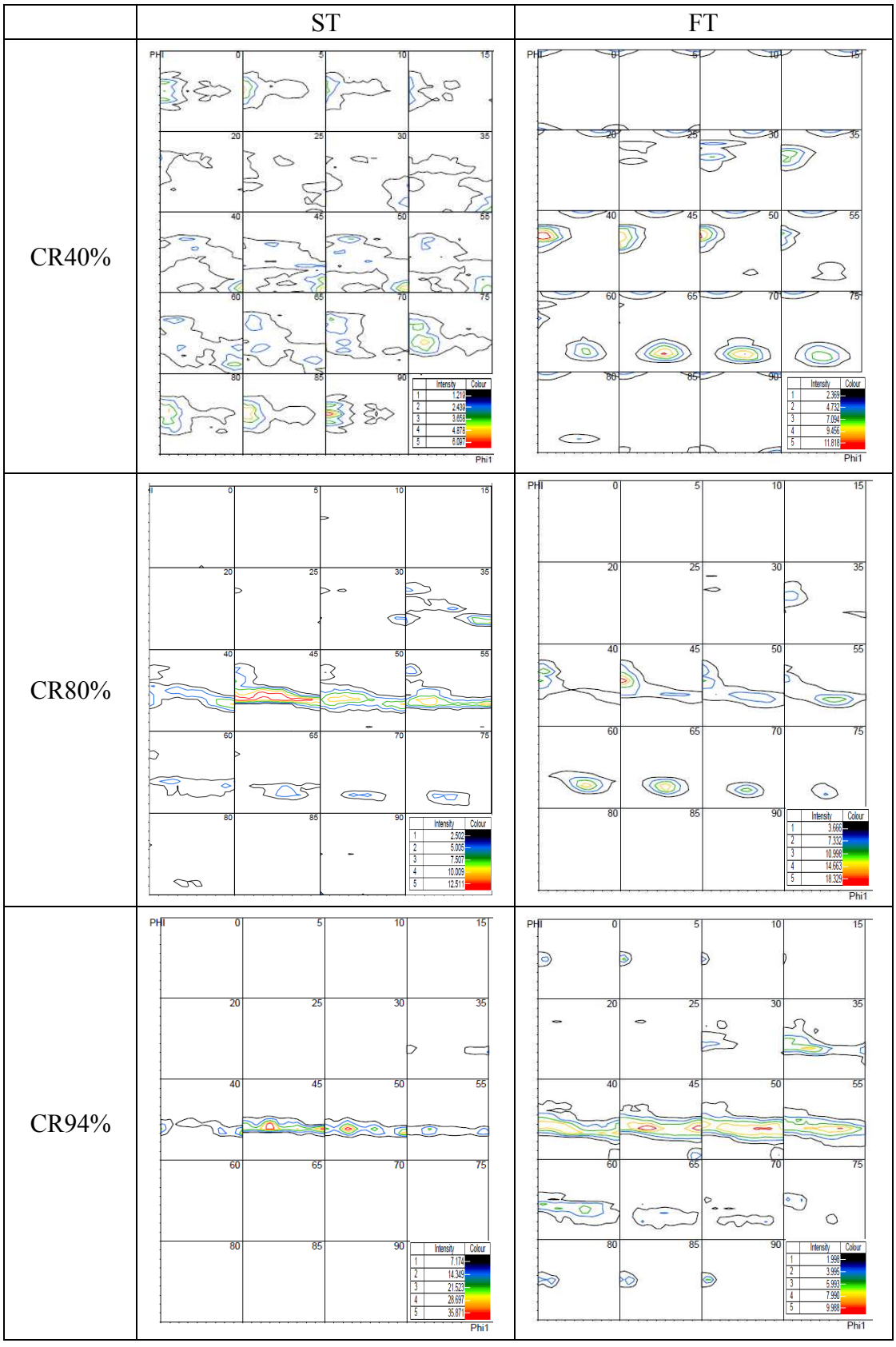

Fig. 6. Constant φ_2 sections of ODF for Ti2448 alloy after different cold rolling rates followed by solution treatment (a, b, c) and flash thermal treatment (d, e, f).

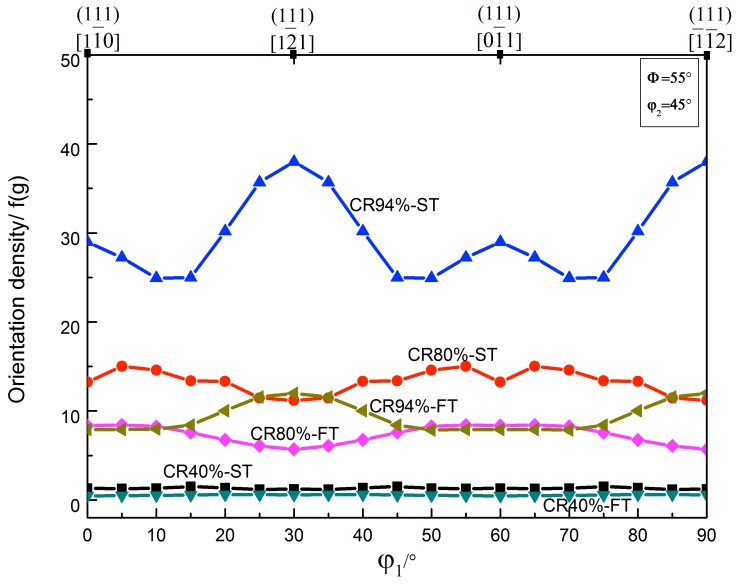

Fig. 7. Orientations distributed along the ϕ=55° line on φ_2=45° sections of ODF observed in specimens after different thermo-mechanical treatments illustrating the presence of γ-fiber.